

1 **Studying the real-time interplay between triglyceride digestion and lipophilic**
2 **micronutrient bioaccessibility using droplet microfluidics. 2 Application to various oils**
3 **and (pro)vitamins**

4 Hoang Thanh NGUYEN, Mélanie MARQUIS, Marc ANTON, Sébastien MARZE

5 Biopolymères Interactions Assemblages, INRA, 44300 Nantes, France

6

7 **Abstract**

8 The kinetics of micellar solubilization of lipophilic micronutrients (bioaccessibility) in relation
9 with triglyceride digestion remains poorly known. To study this interplay in real-time, a droplet
10 microfluidic method was designed and used as reported in the first part of this article series.
11 In this second part, the interplay between the micellar solubilization of (pro)vitamins (beta-
12 carotene or retinyl palmitate) and the digestion of triglyceride oils (tricaprylin TC, or high-oleic
13 sunflower seed oil HOSO, or fish oil FO) during simulated gastrointestinal digestion was
14 investigated. The relation between the release of both micronutrients and of triglyceride
15 lipolytic products was found to be non-linear. The kinetics of beta-carotene was found to
16 follow the kinetics of lipolytic products, depending on the oil type (TC > HOSO > FO). The
17 effect of the gastric phase on the intestinal phase was also found to follow this order, mostly
18 due to partial lipolysis during the gastric phase.

19

20 **1. Introduction**

21 Micronutrients (minerals, vitamins) are essential to maintain normal functions of human body.
22 However, their absorption, especially that of lipophilic vitamins and carotenoids, is much
23 more variable than that of macronutrients, due to biological and physicochemical factors
24 (Borel, 2003). In the fat-soluble micronutrient class, vitamin A has received an intensive
25 research attention due to its multiple functions in normal growth and development of human
26 body. Vitamin A is notably involved in immune system maintenance, vision health and
27 regulation of cell division (Grune et al., 2010; Haskell, 2012). Vitamin A is present in food in
28 two forms: pre-formed vitamin A (mostly as retinyl palmitate) from animal sources, and
29 provitamin A carotenoids (carotenes, beta-cryptoxanthin) from plant sources. Among
30 provitamin A carotenoids, beta-carotene has the highest vitamin A activity thanks to its
31 unique symmetrical structure (Grune et al., 2010; Haskell, 2012). Nevertheless, in order to
32 achieve their vitamin activity, they need to be available in tissues (bioavailability), what
33 requires many processes: i) release from the food matrix and incorporation in triglyceride
34 droplets, ii) co-digestion with triglycerides, then co-solubilization into mixed micelles
35 (bioaccessibility), iii) transport, processing, and secretion by intestinal cells iv) circulation in

36 the lymph or blood system in lipoprotein. Among these processes, the micellar solubilization
37 is an important prerequisite for transport. However, because fat-soluble micronutrients are
38 poorly soluble in the aqueous gastrointestinal environment, their bioaccessibility may be low
39 and variable depending on many factors involving the food matrix structure and composition
40 (Borel, 2003). Improving bioaccessibility is thus a strategy to enhance the bioavailability of
41 these lipophilic micronutrients.

42 For the last couple of decades, many works based on *in vitro* digestion were carried out to
43 study the bioaccessibility of beta-carotene in relation with triglyceride digestion (Huo,
44 Ferruzzi, Schwartz, & Failla, 2007; Yi, Zhong, Zhang, Yokoyama, & Zhao, 2015). However,
45 the interplay between the micellar solubilization of lipophilic micronutrients and of lipolytic
46 products remains poorly known. For that matter, emulsion kinetic studies provided insights
47 into the mechanisms of micellar solubilization of beta-carotene (Borel et al., 1996; Nik,
48 Corredig, & Wright, 2011; Mutsokoti et al., 2017; Verkempinck et al., 2017). Better than a
49 single end-point measurement, the release profile of bioactive molecules can be obtained by
50 analyzing different incubation time points, but this is challenging due to difficulties in the
51 control of experimental parameters using emulsion, the amount of materials needed, and the
52 required high number of time points. Alternative approaches are scarce and the
53 simultaneous real-time kinetics were established only once, using multiplex coherent Anti-
54 Stokes Raman scattering microspectroscopy (Day, Rago, Domke, Velikov, & Bonn, 2010).

55 These issues can also be solved using droplet microfluidics. In the first part of this article
56 series, we proposed a lab on a chip method enabling the simultaneous monitoring of beta-
57 carotene and of tricaprylin lipolytic products in real time. In this second part, we extend this
58 microfluidic approach to other oils and lipophilic micronutrients in order to understand their
59 roles on the kinetic solubilization interplay. Three oils and two (pro)vitamins were tested
60 separately, among which 5 systems were investigated. The full relation between the micellar
61 solubilization of oil lipolytic products and of these micronutrients was established. The effect
62 of the gastric phase on the subsequent intestinal phase was investigated as well.

63

64 **2. Experimental Section**

65 **2.a. Materials**

66 Pancreatic lipase (L3126, lipase from porcine pancreas type II, 1.7-8.3 U mg⁻¹), Amano
67 lipase A (534781, lipase from *Aspergillus niger*, 12 U mg⁻¹, protease activity \leq 2.5 U mg⁻¹),
68 pepsin (P7012, pepsin from porcine gastric mucosa, 2500 U mg⁻¹), sodium
69 glycodeoxycholate (G9910), tricaprylin TC (T9126), beta-carotene (22040), retinyl palmitate

70 RP (R1512) were provided by Sigma-Aldrich. High-oleic sunflower seed oil HOSO was
71 provided by Vandamme (Belgium). Fish oil FO (1050 TG) was provided by Polaris (France).

72 **2.b. Droplet digestion and lipid monitoring**

73 In this work, digestion of oil droplets containing an added micronutrient was performed using
74 the same microfluidic method described in detail in the first part of this article series. Briefly,
75 monodisperse oil droplets of 100 μm containing an added micronutrient were
76 generated/immobilized in a lab on chip device and then subjected to a semi-dynamic
77 gastrointestinal digestion in the same chip, with a continuous flow (and thus renewal) of the
78 digestive fluids at a flow rate of 50 $\mu\text{L min}^{-1}$. The digestion of the trapped oil droplets was
79 carried out under controlled temperature of 37 $^{\circ}\text{C}$ inside the digestion chamber, and
80 monitored in real-time (2 min time steps) using a confocal fluorescence microscope (Nikon
81 A1+) with a 10x objective. All optical parameters were optimized to obtain auto fluorescence
82 intensity of the different micronutrients for quantitative analysis. A laser with an excitation
83 wavelength of 488 nm and a channel with emission window of 500-530 nm were used to
84 obtain the autofluorescence image of BC inside the oil droplets. A transmitted light image for
85 the droplet size was obtained simultaneously using the same excitation beam. Due to its
86 different absorption and emission properties compared to those of BC, a laser with an
87 excitation wavelength of 375 nm and a channel with an emission window of 425-475 nm
88 were used to obtain the autofluorescence image of RP. A transmitted light image for the
89 droplet size was obtained simultaneously using the 488 nm laser already used for BC. The
90 droplet size and fluorescence were measured by image analysis. Micronutrient concentration
91 and release were calculated from these values using a fluorescence calibration curve as
92 explained in the first part of this series.

93 The digestion was run with either an intestinal phase alone or a gastric phase followed by an
94 intestinal phase. The intestinal fluid was prepared by mixing a buffer solution (100 mM
95 NaH_2PO_4 adjusted to pH 7.0) with pancreatic lipase at 4 mg mL^{-1} and a bile salt (sodium
96 glycodeoxycholate) at 5 mg mL^{-1} . When a gastric phase was performed prior to the intestinal
97 phase, it was carried out for 2 hours with a gastric fluid prepared by mixing 0.03 mg mL^{-1}
98 lipase from *Aspergillus niger* (lipase AN), and 0.6 mg mL^{-1} pepsin in a 100 mM KCl buffer
99 adjusted to pH 3.0.

100 Three triglycerides composed of different fatty acids were tested: pure tricaprylin (TC, C8:0),
101 or high-oleic sunflower seed oil (HOSO, mainly C18:1), or a fish oil rich in DHA (FO, mainly
102 C22:6). Two micronutrients were tested separately (same initial concentration of 0.2 wt% in
103 the oils): beta-carotene (provitamin A) or retinyl palmitate (preformed vitamin A). For each
104 system, two to three independent digestions were conducted with the monitoring of seven
105 individual droplets for each digestion. A distinct microfluidic device was used for each

106 digestion to ensure identical initial conditions. The variability of the measurements was very
107 low between the seven droplets monitored during one digestion, so the error bar (plotted as
108 the standard deviation) represents the variability of the two to three independent digestions.

109

110

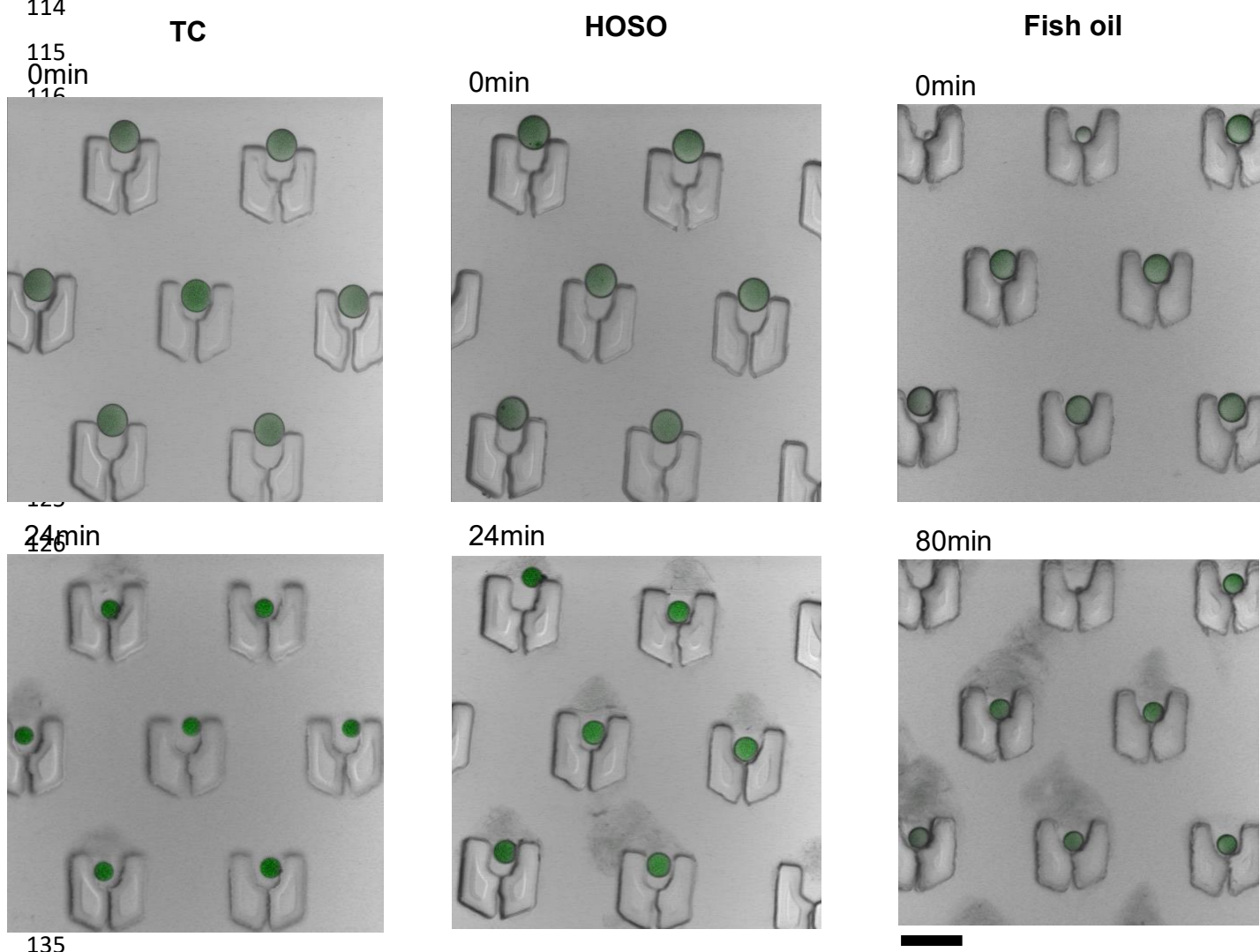
111 3. Results and discussion

112 3.a. Intestinal phase

113

114

115
116



135

136 Fig. 1 Images of droplets containing beta-carotene for different oils (TC, HOSO, fish oil) at
137 various intestinal digestion times. The scale bar represents 200 μm .

138

139

140 Digestion of TC, HOSO, and fish oil containing the same initial BC concentration (0.2 wt%)
141 were conducted. Fig. 1 shows the evolution of droplet size and fluorescence for different oils

142 during the intestinal digestion. The reduction of the droplet size comes from the lipolysis of
143 triglycerides into free fatty acids and monoglycerides, which exit the droplet as they can
144 solubilize in the aqueous bile salt micelles.

145 The digestion kinetics of the three oils is shown in fig. 2a. The fastest rate is found for TC
146 and the slowest rate for fish oil. This is due to higher lipase activity and bile salt solubilization
147 capacity for short saturated fatty acid chains (TC) compared to long polyunsaturated fatty
148 acid chains (fish oil), as already reviewed (Marze, 2014). Calculations were done to quantify
149 the free fatty acid (FFA) release rate during the intestinal digestion. The mathematical model
150 is detailed in the supplementary material S1. Assuming the FFA release rate is proportional
151 to the surface area of the oil droplet (Li & McClements, 2010; Marze & Choimet, 2012;
152 Gaucel, Trelea, & Le Feunteun, 2015), the equation we used reads:

$$153 \quad R(t) = R_0 \left(1 - \frac{k_s M_w}{2R_0 \rho} t \right) \quad (1)$$

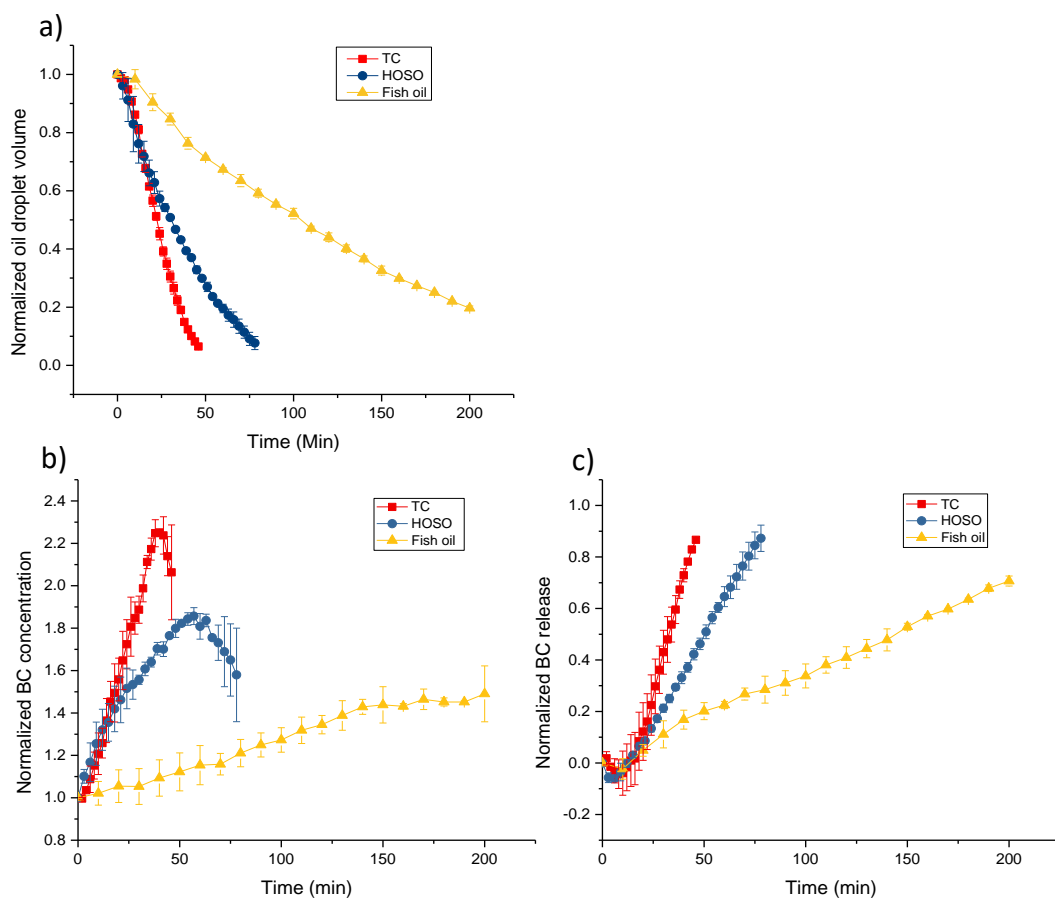
154 where k_s is the FFA release rate per unit droplet surface area ($\text{mol s}^{-1} \text{m}^{-2}$), ρ is the density of
155 the triglyceride oil droplet (g m^{-3}), M_w is the molecular weight of the triglyceride oil (g mol^{-1}), t
156 is the time (s), and R_0 is the initial radius of the oil droplet (m).

157 Note that a similar equation accounting for the total reaction volume is derived in the
158 supplementary material S1. These models were systematically applied to pH-stat
159 measurements of emulsion lipolysis. The comprehensive fitted release rates for microfluidic
160 droplets and for emulsions are compared in the supplementary material S2.

161 The FFA release rate per droplet surface area was determined using eq. (1). The rates were
162 of 41.2 ± 1.4 , 13.2 ± 0.2 , and $3.08 \pm 0.01 \mu\text{mol s}^{-1} \text{m}^{-2}$ for TC, HOSO, and fish oil,
163 respectively. These values are about 35% lower than those obtained previously using droplet
164 microfluidics (Marze, Algaba, & Marquis, 2014), but when the rates are normalized to HOSO,
165 the ratios are of 3.1 and 0.23 for TC and fish oil, respectively, which are close to the ratios of
166 2.5 and 0.21 normalized to olive oil (Marze et al., 2014). The absolute rate values are about
167 one-two orders of magnitude higher than those for emulsions (Li, & McClements, 2010,
168 Marze, & Choimet, 2012, supplementary material S2). This difference is likely due to the
169 absence of coalescence in our droplet microfluidic approach, whereas coalescence reduces
170 the surface area available for lipolysis and solubilization in the case of emulsions, what is not
171 accounted for in the models (supposing no coalescence).

172 The digestion rate also depends on both the lipase specificity for the triglycerides and the
173 capacity of the bile salt to remove the lipolytic products from the droplet surface
174 (solubilization of lipolytic products). In general, the longer the fatty acid chain, the lower the
175 lipase activity and the lower the solubilization capacity for the lipolytic products (Marze,
176 2014). Lipase activity is actually dependent on solubilization capacity, as lipolytic products

177 accumulating at the droplet surface are known to inhibit further lipolysis (Pafumi et al., 2002).
 178 Hence, a lower solubilization capacity will induce a lower apparent lipolysis rate. In these
 179 microfluidic experiments, the continuous renewal of the intestinal fluid results in a large
 180 excess of bile salts, thus lipolysis is likely the limiting step. This is confirmed by comparing
 181 the results of this single droplet study to emulsion lipolysis experiments with optimized bile
 182 salt concentrations (Marze, 2014). The relative rates normalized to HOSO (3.1 and 0.23 for
 183 TC and fish oil, respectively) are indeed in the same range.
 184



185
 186 Fig. 2 a) Evolution of the normalized droplet volume, b) evolution of the normalized BC
 187 concentration inside the droplets, and c) evolution of BC proportion released from the
 188 droplets for different oils (TC, HOSO, Fish oil) during intestinal digestion.

189
 190
 191 In fig. 2b, the concentration of BC in the droplets during intestinal digestion for the three oils
 192 is reported. For TC and HOSO, BC concentration mainly increases during digestion,
 193 reaching a maximum and then decreases near the end of the digestion. For fish oil, the
 194 decreasing part was not observed due to a much longer digestion time. Such increasing
 195 trend for vitamin D3 concentration inside TC droplets was reported for emulsions, but no

196 decrease was observed because the digestions were incomplete (Day et al., 2010). The
197 increase of BC inside the oil droplets could be explained by the competition between BC and
198 lipolytic products for solubilization into the bile salt micelles, knowing that their solubilization
199 capacity is much lower for beta-carotene and retinol (about $5 \cdot 10^{-4}$ and $6 \cdot 10^{-3}$ mol/mol,
200 respectively) (El-Gorab, & Underwood, 1973), compared to fatty acids and monoglycerides
201 (range $4 \cdot 10^{-2}$ – 3.5) (Marze, 2014). Differences in the kinetics of BC concentration for the
202 three oils are observed, as BC concentrates more in the droplets in the case of oils
203 undergoing faster lipolysis.

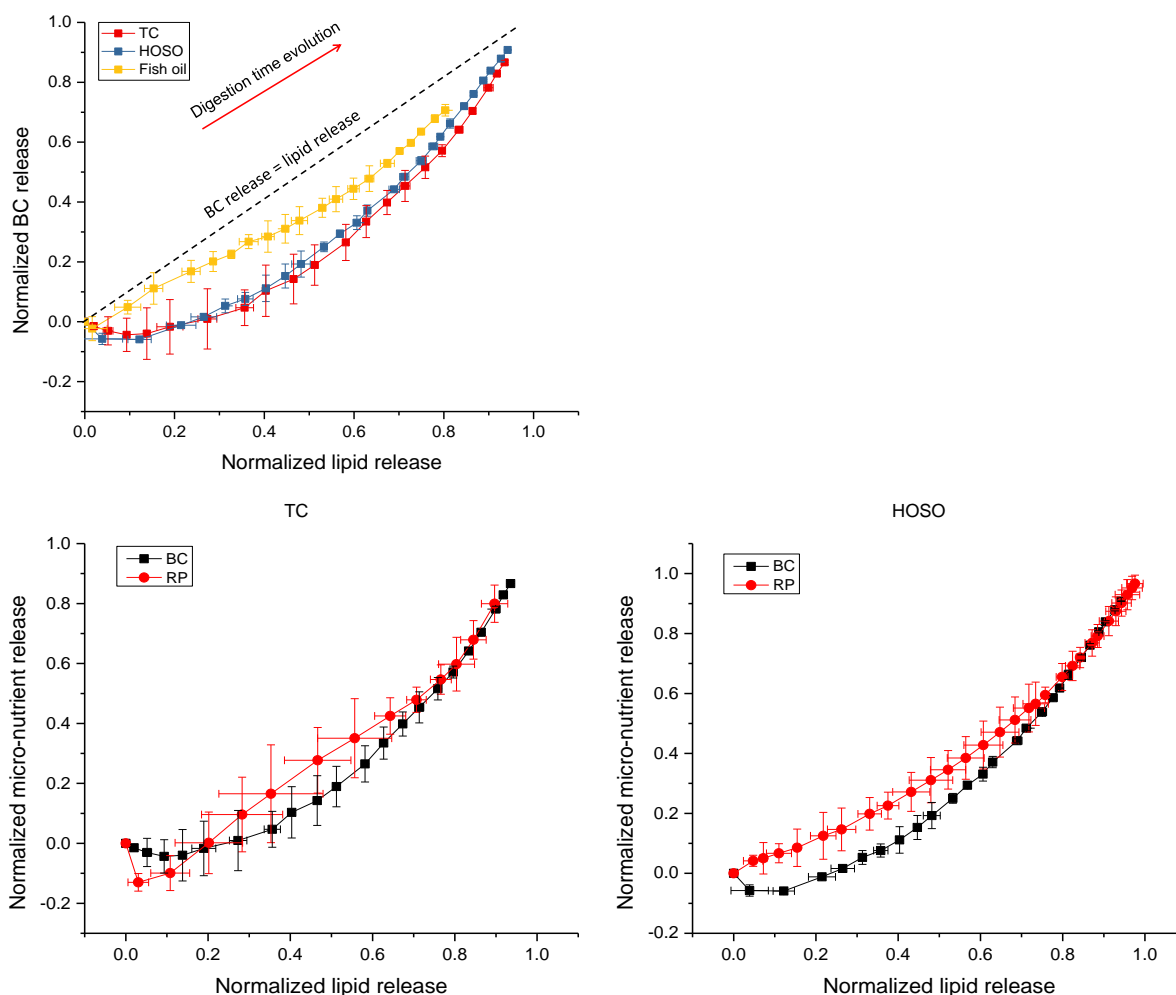
204 The evolution of BC release as a function of intestinal digestion time is presented in fig. 2c.
205 These results show that although BC concentration increases in the droplets, it is
206 nevertheless significantly released in all cases. Thus the concentration increase is due to a
207 slower BC release rate compared to the lipolytic products release rate. The maximal rates of
208 BC release from the oil droplet per unit droplet surface area were calculated from the BC
209 release and the droplet size data, of 0.57 ± 0.04 , 0.25 ± 0.03 , and $0.035 \pm 0.008 \mu\text{mol s}^{-1} \text{m}^{-2}$
210 for TC, HOSO, and fish oil, respectively. The BC release rates were found to follow the same
211 order as the lipolytic products release rates (TC > HOSO > FO). This is in agreement with
212 many studies showing higher bioaccessibility of various lipophilic compounds from medium-
213 chain triglycerides compared to long-chain triglycerides (Marze, 2015). For all three oils,
214 much higher final BC bioaccessibility values (about 90% in the cases of the fully digested TC
215 and HOSO) were found compared to values obtained for the static digestion of emulsions in
216 the literature (Nik et al., 2011; Mutsokoti et al., 2017; Verkempinck et al., 2017). This is likely
217 explained by the continuous renewal of the intestinal digestive fluid (semi-dynamic method),
218 providing bile salt micelles that are not saturated with lipolytic products and BC constantly, in
219 contrast with the static methods in which saturated bile salt micelles are not replaced. Note
220 that a porcine bile extract containing various bile salts was also tested instead of the single
221 bile salt, at the same total bile salt concentration. The kinetics were found to be significantly
222 faster only in the case of TC, probably because all bile salts formed mixed micelles efficiently
223 with medium-chain fatty acids and monoglycerides, as compared to long-chain ones (Marze,
224 2014).

225 As in the first article of this series, the relation between the micellar solubilization of BC and
226 of the lipolytic products is shown in fig. 3. First, we observe that this relation is almost linear
227 in the case of fish oil, but can be highly non-linear in the cases of TC and HOSO. The added
228 black dash line represents the “balance” case in which the BC release equals the lipolytic
229 products release (also named lipid release). All three curves lie below this black dash line, so
230 the relative mass release of BC is always lower compared to that of lipids, hence the
231 increase of the BC concentration inside the oil droplets observed in fig. 2b. Although the BC
232 release rate ranks like the lipid release rate, that is TC > HOSO > FO, the reverse is true

233 when BC mass release is compared to the lipid mass release. The curve of fig. 3 can be
234 seen as a micronutrient release efficiency curve, where the closer the curve from the black
235 dash line, the more efficient the triglyceride digestion is for BC release.

236 For retinyl palmitate, RP concentration trends inside the oil droplets and RP release were
237 very similar to those for BC shown in figs. 2. The final RP release efficiency curves for two
238 oils are compared to the case of BC in figs. 3b and 3c. The results show similar non-linear
239 relations. A higher RP release efficiency compared to BC is observed in the first part of the
240 digestion. However, this is only statistically significant in the case of HOSO due to much
241 larger error bars for RP. These variations were explained by much larger fluctuations in the
242 intensity of the 375 nm laser as compared to the 488 nm laser.

243



244

245 Fig. 3 a) Relation between the normalized mass release of BC and of lipids for different oils
246 (TC, HOSO, fish oil), b) comparison between BC and RP release for TC, and c) comparison
247 between BC and RP release for HOSO.

248

249

250 In the case of a fast initial lipolysis (TC and HOSO), the micronutrients must compete with
251 more lipolytic products for solubilization in bile salt micelles. Thus, it leads to a low initial BC
252 mass release. The curve for the fish oil is significantly different, showing that a slower initial
253 lipolysis can induce a high initial BC mass release. In this case, there is more interplay
254 between micronutrient release and lipid digestion, suggesting that cooperation prevails over
255 competition. This is in agreement with the enhancement of the solubilization capacity of bile
256 salt micelles by the formation of mixed micelles containing fatty acids and monoglycerides.
257 This enhancement is indeed known to be much more efficient in the case of long
258 polyunsaturated lipids compared to short saturated ones (Kossena, 2004). This could be
259 understood on the basis of the formation of highly swollen mixed micelles accommodating
260 large lipophilic molecules, or poorly swollen mixed micelles with lower solubilization capacity,
261 respectively (Colle, 2012).

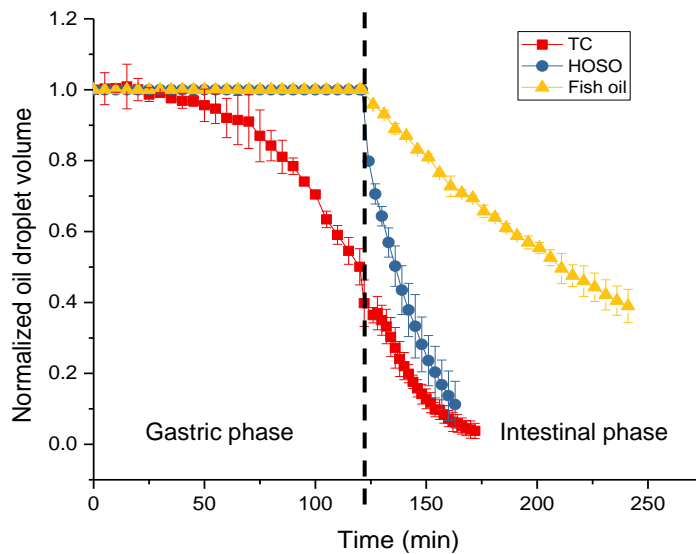
262 Similar to the case for TC discussed in the first article of the series, the BC release efficiency
263 curve for HOSO was found to be non-linear with three different kinetic regimes. In contrast,
264 strictly linear relations are often reported in emulsion digestion studies (Borel et al., 1996; Nik
265 et al., 2011; Mutsokoti et al., 2017). This is likely due to the limited number of time points
266 monitored using the emulsion approach. Indeed, most portions of the full efficiency curve will
267 appear linear with scarce data points. In the contrary, very similar non-linear curves were
268 obtained from agent-based simulations (Marze, 2014). In addition to the
269 competition/cooperation interpretation, these simulations revealed that highly lipophilic
270 molecules slowly diffuse inside the droplet. When the triglyceride digestion rate is slow, they
271 statistically have enough time to reach the interface at the beginning of the digestion (ideal
272 balance case and fish oil). When the triglyceride digestion rate is fast, they statistically reach
273 the interface towards the end of the digestion, when the droplet size is small, hence the
274 higher release in this regime.

275

276 **3.b. Effect of the gastric phase**

277 A gastric phase was added prior to the intestinal phase in order to investigate its effect. Fig. 4
278 shows the evolution of the normalized droplet volume as a function of digestion time during
279 the gastric phase followed by the intestinal phase for the three oils. During the gastric phase,
280 a decrease in the droplet volume was only observed for TC. Using eq. (1), the release rate of
281 FFA per unit droplet surface area was calculated to be $9.7 \pm 2.8 \mu\text{mol s}^{-1} \text{m}^{-2}$, which is much
282 lower than that during the intestinal phase ($41.2 \pm 1.4 \mu\text{mol s}^{-1} \text{m}^{-2}$). These results are
283 consistent with those reported by Marze et al., 2014 and can be explained by the much lower
284 concentration of lipase AN compared to pancreatic lipase, and by the absence of bile salts in

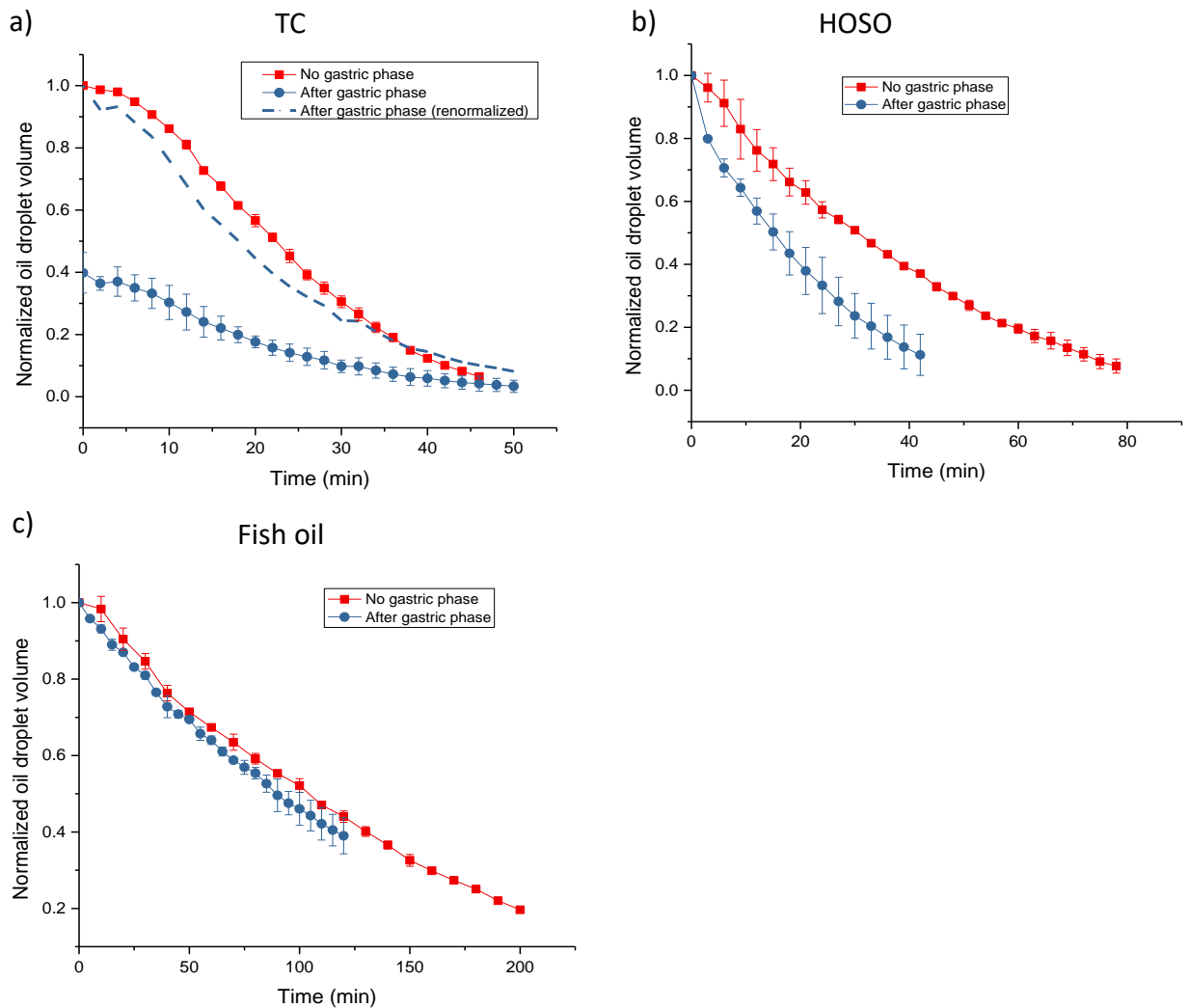
285 the gastric phase. The lipolytic products of TC have a sufficiently high aqueous solubility to
286 be removed from the interface in the absence of bile salt micelles, allowing interfacial lipase
287 activity. In the contrary, the poorly water soluble lipolytic products of long-chain triglycerides
288 (HOSO and fish oil) can actually not be solubilized in the aqueous phase and hence saturate
289 the interface, allowing only partial lipolysis by inhibiting further lipase activity (Pafumi et al.,
290 2002).
291



292
293 Fig. 4 Evolution of the normalized droplet volume for different oils (TC, HOSO, fish oil) as a
294 function of digestion time, with a gastric phase before the intestinal phase.

295
296
297 In figs. 5, the evolution of the droplet volume during the intestinal phase (with or without a
298 preceding gastric phase) is presented. It shows that the effect of the gastric phase depends
299 on the oil. The shorter the chain length of the triglycerides is, the greater the effect. In the
300 case of TC, the gastrointestinal digestion extent was always higher than the intestinal
301 digestion alone, mainly due to the solubilization during the gastric phase. Indeed, when the
302 droplet volume is renormalized at the start of the intestinal phase, the kinetics is only
303 significantly faster at the beginning of the intestinal phase, with an initial steep decrease in
304 the droplet volume. In the case of HOSO, an even steeper decrease is observed at the
305 beginning of the intestinal phase following the gastric phase. This confirms that partial
306 lipolysis occurred and lipolytic products accumulated at the droplet interface during the
307 gastric phase, immediately removed by the bile salt micelles at the start of the intestinal
308 phase, causing the steep decrease in the droplet volume. In the contrary, the gastric phase
309 has almost no effect in the case of the fish oil. Those results are different from the ones

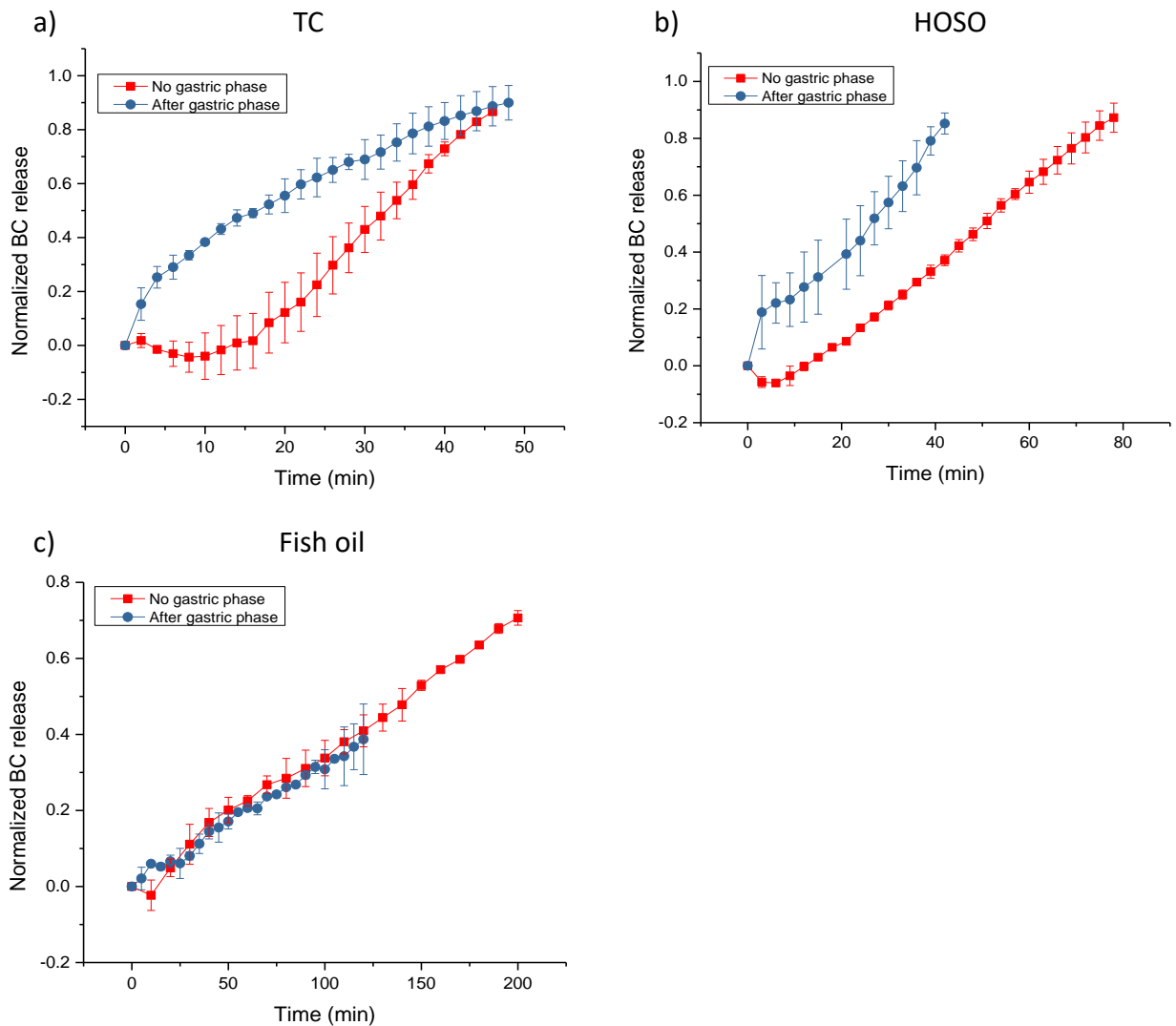
310 reported by Marze et al., 2014, in which the gastric phase had no effect on the following
 311 intestinal phase. This contradiction can be explained by different experimental parameters
 312 regarding the initial droplet size, the gastric fluid composition, and the gastric phase duration.
 313 In the current experiments, the initial droplet size was smaller (higher surface to volume
 314 ratio), pepsin was present in the gastric fluid, hydrolyzing the initial layer of beta-
 315 lactoglobulin, and the gastric phase duration was longer.
 316



317
 318 Fig. 5 Effect of the gastric phase on the intestinal phase of digestion for different oils: a) TC,
 319 b) HOSO, c) fish oil.

320
 321
 322 Figs. 6 show the effect of the gastric phase on the BC release from the oil droplets during the
 323 intestinal phase. For TC and HOSO, the BC release is significantly faster at the beginning of
 324 the intestinal phase when a preceding gastric phase was performed. For TC, this is likely due
 325 to the smaller size of the droplets, as discussed above. For HOSO, BC molecules could

326 localize in clusters of lipolytic products at the droplet surface, as postulated by Pafumi et al.,
327 2002 for long-chain lipids. When the intestinal phase starts, the bile salt micelles would
328 quickly solubilize these clusters, resulting in a fast release of both lipids and BC. For fish oil,
329 no effect of the gastric phase on the BC release during the intestinal phase was observed.
330



331
332 Fig. 6 Effect of the gastric phase on BC release from the droplets during the intestinal phase
333 of digestion for different oils: a) TC, b) HOSO, c) fish oil.
334

335
336 **Conclusion**

337 The full kinetic relation between the release of micronutrients and the release of lipolytic
338 products was found to be non-linear for both BC and RP. The bioaccessibility kinetics of both
339 micronutrients depended on the type of fatty acid. BC added to the quickly digested oil (TC,
340 with a short saturated fatty acid chain) presented a lower release efficiency compared to BC

341 added in the slowly digested oil (fish oil, with long polyunsaturated fatty acid chains). The
342 interplay between the bioaccessibility of micronutrients and the lipolysis of triglycerides was
343 interpreted on the basis of micellar solubilization competition/cooperation and of
344 digestion/diffusion time comparisons. The effect of the gastric phase before the intestinal
345 phase was also found to depend on the fatty acid type.
346 These results could be used to design delivery systems with controlled release properties
347 based on the oil-micronutrient association. Overall, these results show the need for real-time
348 kinetics studies of lipophilic micronutrients to provide insights about their fate in the
349 gastrointestinal tract. This knowledge will enable a better understanding and improvement of
350 the bioaccessibility of lipophilic micronutrients, and in turn could prove essential to control
351 their bioavailability.

352

353 **References**

- 354 Borel, P. (2003). Factors affecting intestinal absorption of highly lipophilic food
355 microconstituents (fat-soluble vitamins, carotenoids and phytosterols). *Clinical*
356 *Chemistry and Laboratory Medicine*, 41(8), 979–994.
- 357 Borel, P., Grolier, P., Armand, M., Partier, A., Lafont, H., Lairon, D., & Azais-Braesco, V.
358 (1996). Carotenoids in biological emulsions: Solubility, surface-to-core distribution, and
359 release from lipid droplets. *Journal of Lipid Research*, 37(2), 250–261.
- 360 Colle, I. J. P., Van Buggenhout, S., Lemmens, L., Van Loey, A. M., & Hendrickx, M. E.
361 (2012). The type and quantity of lipids present during digestion influence the in vitro
362 bioaccessibility of lycopene from raw tomato pulp. *Food Research International*, 45(1),
363 250–255.
- 364 Day, J. P. R., Rago, G., Domke, K. F., Velikov, K. P., & Bonn, M. (2010). Label-free imaging
365 of lipophilic bioactive molecules during lipid digestion by multiplex coherent anti-stokes
366 raman scattering microspectroscopy. *Journal of the American Chemical Society*,
367 132(24), 8433–8439.
- 368 El-Gorab, M., & Underwood, B. A. (1973). Solubilization of beta-carotene and retinol into
369 aqueous solutions of mixed micelles, 306, 58–66.
- 370 Giang, T. M., Gaucel, S., Brestaz, P., Anton, M., Meynier, A., Trelea, I. C., & Le Feunteun, S.
371 (2016). Dynamic modeling of in vitro lipid digestion: individual fatty acid release and
372 bioaccessibility kinetics. *Food Chemistry*, 194, 1180–1188.
- 373 Grune, T., Lietz, G., Palou, A., Ross, A. C., Stahl, W., Tang, G., ... Biesalski, H. K. (2010).
374 Beta-carotene is an important vitamin A source for humans. *The Journal of Nutrition*,
375 140(12), 2268S–2285S.
- 376 Haskell, M. J. (2012). The challenge to reach nutritional adequacy for vitamin A: β -carotene
377 bioavailability and conversion - Evidence in humans. *American Journal of Clinical*

378 *Nutrition*, 96(5), 1193S-1203S.

379 Huo, T., Ferruzzi, M. G., Schwartz, S. J., & Failla, M. L. (2007). Impact of fatty acyl
380 composition and quantity of triglycerides on bioaccessibility of dietary carotenoids.
381 *Journal of Agricultural and Food Chemistry*, 55(22), 8950–8957.

382 Kossena, G. A., Charman, W. N., Boyd, B. J., Dunstan, D. E., & Porter, C. J. H. (2004).
383 Probing Drug Solubilization Patterns in the Gastrointestinal Tract after Administration of
384 Lipid-Based Delivery Systems: A Phase Diagram Approach. *Journal of Pharmaceutical*
385 *Sciences*, 93(2), 332–348.

386 Li, Y., & McClements, D. J. (2010). New mathematical model for interpreting pH-stat digestion
387 profiles: Impact of lipid droplet characteristics on in vitro digestibility. *Journal of*
388 *Agricultural and Food Chemistry*, 58(13), 8085–8092.

389 Marze, S., & Choimet, M. (2012). In vitro digestion of emulsions: Mechanistic and
390 experimental models. *Soft Matter*, 8(42), 10982–10993.

391 Marze, S. (2014). A coarse-grained simulation to study the digestion and bioaccessibility of
392 lipophilic nutrients and micronutrients in emulsion. *Food Funct.*, 5(1), 129–139.

393 Marze, S., Algaba, H., & Marquis, M. (2014). A microfluidic device to study the digestion of
394 trapped lipid droplets. *Food Funct.*, 5(7), 1481–1488.

395 Mutsokoti, L., Panozzo, A., Pallares Pallares, A., Jaiswal, S., Van Loey, A., Grauwet, T., &
396 Hendrickx, M. (2017). Carotenoid bioaccessibility and the relation to lipid digestion: A
397 kinetic study. *Food Chemistry*, 232, 124–134.

398 Nik, A. M., Corredig, M., & Wright, A. J. (2011). Release of lipophilic molecules during in vitro
399 digestion of soy protein-stabilized emulsions. *Molecular Nutrition and Food Research*,
400 55(SUPPL. 2), 278–289.

401 Pafumi, Y., Lairon, D., De La Porte, P. L., Juhel, C., Storch, J., Hamosh, M., & Armand, M.
402 (2002). Mechanisms of inhibition of triacylglycerol hydrolysis by human gastric lipase.
403 *Journal of Biological Chemistry*, 277(31), 28070–28079.

404 Yi, J., Zhong, F., Zhang, Y., Yokoyama, W., & Zhao, L. (2015). Effects of Lipids on in Vitro
405 Release and Cellular Uptake of β -Carotene in Nanoemulsion-Based Delivery Systems.
406 *Journal of Agricultural and Food Chemistry*, 63(50), 10831–10837.

407

Mathematical models for the FFA release

Calculations were done to quantify the free fatty acid (FFA) release rate during the intestinal digestion. Assuming the FFA release rate is proportional to the surface area of the oil droplet (Li & McClements, 2010; Marze & Choimet, 2012; Gaucel et al., 2015), the number of moles of FFA released from the droplet per unit time (mol s^{-1}) is written:

$$\frac{dN_{FFA}}{dt} = k_s S \quad (1)$$

where S is the droplet surface area (m^2), and k_s is the FFA release rate per unit droplet surface area ($\text{mol s}^{-1} \text{m}^{-2}$).

As the lipolysis of one triglyceride (TG) molecule releases two molecules of free fatty acid (and one molecule of monoglyceride):

$$\frac{dN_{FFA}}{dt} = -2 \frac{dN_{TG}}{dt} \quad (2)$$

where $\frac{dN_{TG}}{dt}$ is the number of moles of TG lost from the oil droplet per unit time due to lipolysis and solubilization, with N_{TG} the number of TG moles in the oil droplet (mol).

From eqs (1), (2) we have

$$k_s S = -2 \frac{dN_{TG}}{dt} \quad (3)$$

The number of TG moles can be related to the droplet volume as:

$$N_{TG} = \frac{V \rho}{M_w} \quad (4)$$

where V is the volume of the triglyceride oil droplet (m^3), ρ is the density of the triglyceride oil droplet (g m^{-3}), assumed to be constant throughout digestion, and M_w is the molecular weight of the triglyceride oil (g mol^{-1}).

From eqs. (3) and (4), we have:

$$k_s S = -2 \frac{\rho}{M_w} \frac{dV}{dt} \quad (5)$$

as $S = 4\pi R^2$ and $V = \frac{4}{3}\pi R^3$, R being the radius of the oil droplet (m). Substituting S and V in eq. (5) leads to:

$$k_S 4\pi R^2 = -2 \frac{\rho}{M_W} \frac{dV}{dR} \frac{dR}{dt} = -2 \frac{\rho}{M_W} 4\pi R^2 \frac{dR}{dt} \quad (6)$$

Simplifying eq. (6) leads to:

$$k_S = -2 \frac{\rho}{M_W} \frac{dR}{dt} \quad (7)$$

for which a solution can be calculated to be:

$$R(t) = R_0 \left(1 - \frac{k_S M_W}{2R_0 \rho} t \right) \quad (8)$$

For $N_{FFA}(t)$, a solution was calculated in the literature (Li & McClements, 2010; Marze & Choimet, 2012; Gaucel et al., 2015):

$$N_{FFA}(t) = 2N_{TG, total} \left[1 - \left(1 - \frac{k_S M_W}{2R_0 \rho} t \right)^3 \right] \quad (9)$$

Assuming the FFA release rate is proportional to the surface area of the oil droplet per unit total reaction volume (specific surface area), eqs. (8) and (9) can be rewritten as:

$$R(t) = R_0 \left(1 - \frac{k_{SV} M_W}{2R_0 \rho V_T} t \right) \quad (10)$$

$$N_{FFA}(t) = 2N_{TG, total} \left[1 - \left(1 - \frac{k_{SV} M_W}{2R_0 \rho V_T} t \right)^3 \right] \quad (11)$$

where V_T is the total reaction volume (m^3), that is the volume of both the oil and the aqueous phases, and k_{SV} is the FFA release rate per unit specific droplet surface area ($mol\ m\ s^{-1}$).

References

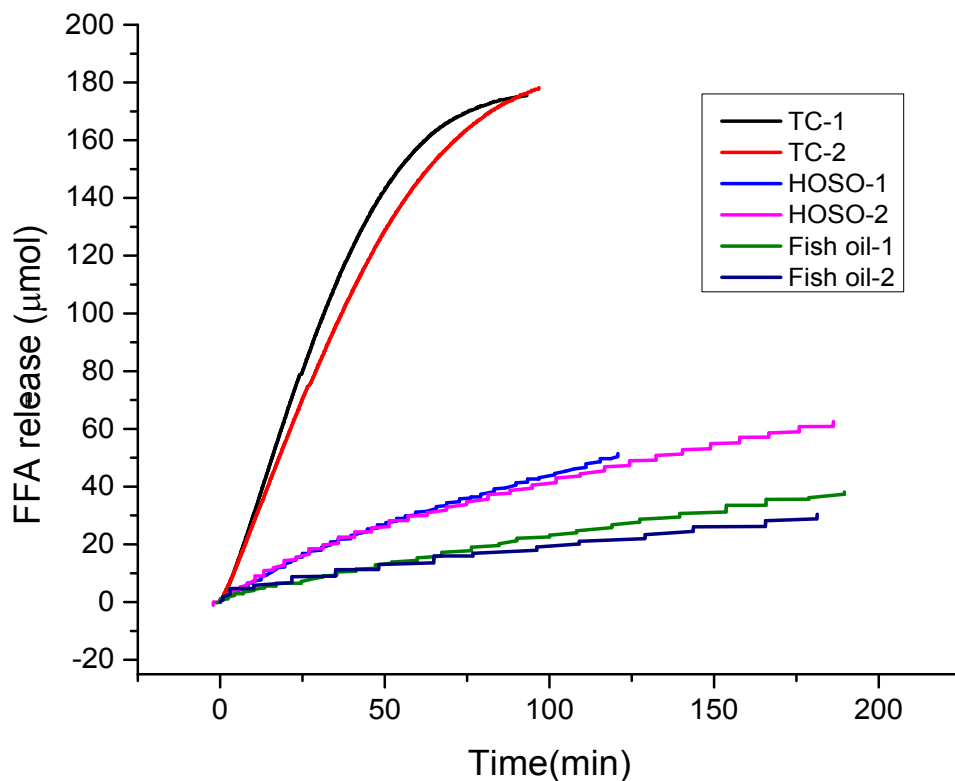
- Li, Y., & McClements, D. J. (2010). New mathematical model for interpreting pH-stat digestion profiles: Impact of lipid droplet characteristics on in vitro digestibility. *Journal of Agricultural and Food Chemistry*, 58(13), 8085–8092.
- Marze, S., & Choimet, M. (2012). In vitro digestion of emulsions: Mechanistic and experimental models. *Soft Matter*, 8(42), 10982–10993.
- Gaucel, S., Trelea, I. C., & Le Feunteun, S. (2015). Comment on New Mathematical Model for Interpreting pH-Stat Digestion Profiles: Impact of Lipid Droplet Characteristics on in Vitro Digestibility, 3(4), 4–5.

pH-stat measurements for emulsions

The digestion degree of emulsions was measured by the pH-stat method with buffer and ionization corrections (Chatzidaki et al., 2016).

Emulsions (2 wt% oil) of different oils (TC or HOSO or fish oil) were prepared. The aqueous phase (2 mg mL^{-1} beta-lactoglobulin) was prepared by mixing the protein in $10 \text{ mM NaH}_2\text{PO}_4$ buffer solution (pH 7.0) for 30 min at room temperature. A rotor-stator homogenizer (Silent Crusher M, Heidolph Instruments, Germany) was used for a pre-emulsification step (2 min, 16000 rpm). Then, a fine emulsion was obtained by sonication (Misonix Sonicator 4000, Qsonica, USA) applied for 3 cycles of 1 min (total energy 2100 J). A 2 min cooling time was applied between each cycle. The droplet size distributions of the emulsions were measured using dynamic light scattering (Zetasizer Nano ZS, Malvern Instruments, UK) equipped with a He-Ne laser of wavelength 633 nm. The volume-based mean droplet diameters were found to be of 265 ± 38 , 313 ± 43 , and 351 ± 48 nm for TC, HOSO, and fish oil emulsions, respectively.

Emulsions were diluted 2 fold with a gastric buffer solution (130 mM NaCl , $1.6 \text{ mM CaCl}_2 \cdot (\text{H}_2\text{O})_2$, pH 3.0) to mimic the gastric dilution. The digestion was started by diluting the gastric emulsion 2 fold in the intestinal fluid (130 mM NaCl , $1.6 \text{ mM CaCl}_2 \cdot (\text{H}_2\text{O})_2$, pH 7.0) containing 0.2 mg mL^{-1} pancreatic lipase (L3126) and 20 mg mL^{-1} bile extract (B8631, about 50 wt% bile salts). FFA release was measured in duplicate with a pH-stat titrator at $37 \text{ }^\circ\text{C}$ (TitraLab 90, Radiometer, Denmark). The results are shown in the figure below.



FFA release during intestinal digestion for different oils in emulsion, measured by the pH-stat method.

By fitting these data with eq. (9) of supplementary material S3, we obtained the FFA release rate per unit surface area, which we compared to the values obtained for the microfluidic experiments (table 1). The values for the pH-stat are in good agreement with our previous results (Marze, & Choimet, 2012), but much lower than those reported by Li and McClements (2010). This is likely related to the much lower concentrations of lipase and calcium we used compared to these authors. It is indeed known that the lipolysis rate is increased by both lipase and calcium concentrations. The pH-stat values are also much lower than the microfluidic values. As already discussed, this can be due to a coalescence process for emulsions, but it is unlikely to explain alone such a large difference.

Table 1: FFA release rate per unit surface area of the oil droplets.

Oil	FFA release rate by the pH-stat method ($\mu\text{mol s}^{-1} \text{m}^{-2}$)	FFA release rate by the microfluidic method ($\mu\text{mol s}^{-1} \text{m}^{-2}$)
TC	$68 \times 10^{-3} \pm 7 \times 10^{-3}$	41.2 ± 1.4
HOSO	$10.5 \times 10^{-3} \pm 0.8 \times 10^{-3}$	13.2 ± 0.2
Fish oil	$5.1 \times 10^{-3} \pm 0.8 \times 10^{-3}$	3.08 ± 0.01

The pH-stat data were also fitted with eq. (11) of supplementary material S3 to evaluate the effect of the total reaction volume. The FFA release rate per unit specific surface area are compared in table 2 with the values fitted for the microfluidic experiments using eq. (10). The values are now much closer (related by a factor 2.4, or in the same range for HOSO). It is thus clear that the total reaction volume is an essential parameter to compare experiments at different scales.

Table 2: FFA release rate per unit specific surface area of the oil droplets.

Oil	FFA release rate by the pH-stat method ($\mu\text{mol } \mu\text{L s}^{-1} \text{m}^{-2}$)	FFA release rate by the microfluidic method ($\mu\text{mol } \mu\text{L s}^{-1} \text{m}^{-2}$)
TC	544 ± 56	226.6 ± 7.7
HOSO	84.0 ± 6.4	72.6 ± 1.1
Fish oil	40.8 ± 6.4	16.94 ± 0.06

Finally, we analyzed the pH-stat data by the standard enzyme activity calculation, using the initial maximal slope ($\mu\text{mol min}^{-1}$) of the FFA release curve, normalized by the mass of lipase in the reaction volume ($\mu\text{mol FFA min}^{-1} \text{mg}^{-1}$ lipase, usually abbreviated to U mg^{-1}). The value of 0.84 U mg^{-1} for HOSO is about 2 fold lower than the minimal value reported by the manufacturer for olive oil. This result is nevertheless reasonable as the protocol of the manufacturer (Sigma) is unknown except for the pH which is 7.7, but overall should be similar.

Knowing the total number of moles of TG in the reaction volume, we also calculated a maximal molar percentage ($\% \text{ min}^{-1}$) of FFA release from the initial maximal slope. To compare with the microfluidic data, we derived an equation based on the same assumption:

$$\frac{dN_{FFA}}{dt} = kN_{FFA,total} = -2 \frac{dN_{TG}}{dt} = -2kN_{TG,total} \quad (1)$$

As $N_{TG,total} = \frac{V_0 \rho}{M_W}$, then we have:

$$\frac{dV}{dt} = kV_0 \quad (2)$$

which we can integrate to find:

$$V(t) = V_0(1 - kt) \quad (3)$$

where k is the FFA release rate (in min^{-1}). Eq. (3) was used to fit the maximal slope in the decrease of the normalized droplet volume, multiplied by 100 to obtain the value in $\% \text{ min}^{-1}$. The maximal BC release rate was also calculated by using the maximal slope of the normalized release curve, converted to $\% \text{ min}^{-1}$. The results are given in table 3, showing that this simple model, although not representing correctly the release curves that are not strictly linear, reconciles the data for both experiments. This means that the release rate in mol min^{-1} can be seen as driven by the total amount of TG, faster for a higher amount. The maximal BC release is also found to have similar values in $\% \text{ min}^{-1}$, not significantly different from those for FFA in the microfluidic experiments, and in the same range than that reported by Mutsokoti et al. (2017). Although the whole real-time kinetics of FFA and BC release were found to be distinct, using the maximal rate values confirms that some specific regimes obey the same kinetics.

Table 3: Maximal lipase activity and FFA release rate for the pH-stat experiments, FFA and BC release rates for the microfluidic experiments.

Oil	Maximal lipase activity by the pH-stat method ($\mu\text{mol FFA min}^{-1} \text{ mg}^{-1}$ lipase)	Maximal FFA release rate by the pH-stat method ($\% \text{ min}^{-1}$)	Maximal FFA release rate by the microfluidic method ($\% \text{ min}^{-1}$)	Maximal BC release rate by the microfluidic method ($\% \text{ min}^{-1}$)
TC	3.7 ± 0.3	1.8 ± 0.2	2.8 ± 0.2	3.0 ± 0.4
HOSO	0.84 ± 0.01	0.71 ± 0.01	1.3 ± 0.2	1.42 ± 0.02
Fish oil	0.27 ± 0.03	0.38 ± 0.03	0.45 ± 0.07	0.55 ± 0.15

References

- Li, Y., & McClements, D. J. (2010). New mathematical model for interpreting pH-stat digestion profiles: Impact of lipid droplet characteristics on in vitro digestibility. *Journal of Agricultural and Food Chemistry*, 58(13), 8085–8092.
- Marze, S., & Choimet, M. (2012). In vitro digestion of emulsions: Mechanistic and experimental models. *Soft Matter*, 8(42), 10982–10993.
- Chatzidaki, M. D., Mateos-Diaz, E., Leal-Calderon, F., Xenakis, A., & Carrière, F. (2016). Water-in-oil microemulsions versus emulsions as carriers of hydroxytyrosol: an in vitro gastrointestinal lipolysis study using the pHstat technique. *Food Funct.*, 7(5), 2258–2269.
- Mutsokoti, L., Panozzo, A., Pallares Pallares, A., Jaiswal, S., Van Loey, A., Grauwet, T., & Hendrickx, M. (2017). Carotenoid bioaccessibility and the relation to lipid digestion: A kinetic study. *Food Chemistry*, 232, 124–134.